Cavity Ring-Down Spectroscopy Measurements of Trace H_2S in SF_6 and SF_6/N_2 Mixture

*ZOU Keyuan, ZHU Min, ZHANG Chaohai**

College of Automation Engineering, Nanjing University of Aeronautics and Astronautics, Nanjing 211106, P.R. China

(Received 15 April 2022; revised 20 June 2022; accepted 10 July 2022)

Abstract: H_2S is one of the most important characteristic decomposition components of SF_6 insulated gas, and the detection of trace H_2S is significant for early fault diagnosis of gas insulated electrical equipment. A 1 578 nm wavelength distributed feedback diode laser (DFB-DL) based cavity ring-down spectroscopy (CRDS) experimental platform is developed to monitor the concentrations of H_2S in SF_6 and SF_6/N_2 mixture carrier gas. The detection sensitivity is higher than 1×10^{-6}. The absorption cross section parameter σ is vital for calculating the concentration. With repeated experiments using standard gas samples, parameter σ of H_2S in pure SF_6 and SF_6/N_2 mixture carrier with different mixing ratios is calibrated. Compared with the simulated σ values, the influence of carrier gas on the broadening of spectral profile is discussed. The variation of absorption cross section σ with different carrier gas mixing ratios is studied as well, so that the calculation of the concentration in the carrier gas of any mixing ratio is possible. Thus, the application of CRDS in trace component detection of gas insulated electrical equipment is promising.

Key words: cavity ring-down spectroscopy (CRDS); absorption cross section; H_2S; SF_6 decomposition component

CLC number: O433 **Document code:** A **Article ID:** 1005-1120(2022)S-0113-07

0 Introduction

Due to the excellent insulation and arc extinguishing performance, SF_6 and its mixed gas insulated electrical equipment cover almost the whole power transmission and transformation field and occupies an absolute dominant position. However, during the process of production, operation and maintenance, insulation defects such as burrs, free metal particles and suspended potential will inevitably appear in the SF_6 insulated electrical equipment. With the extension of operation time and the improvement of voltage level, the extremely uneven electric field reasoned by internal defects of SF_6 gas insulated switchgear will cause partial discharge (PD), which make SF_6 decompose into low fluorine sulfur compounds and then react with trace water and oxygen to form a range of decomposition products, including CO, CO_2, CF_4, C_2F_6, SOF_2, SO_2F_2, SO_2, H_2S, CS_2 and so on[1-2]. As this process induces further insulation deterioration, the safe operation of the whole power grid will be threatened as well.

In order to monitor the insulation status of SF_6 insulated electrical equipment[3-4], the electrical method such as ultrasonic and UHF measurement of partial discharge and chemical diagnosis method based on the characteristic decomposition products of partial discharge SF_6 have been widely used in China's power grid[5-6]. Unlike electrical methods which directly measures signal of PD, chemical method as an indirect way of defect analysis applies gas analysis equipment of great sensibility and accuracy, real-time is also necessary, otherwise the fault early warning will be impossible.

H_2S is one of the characteristic products of SF_6[7] and acts as a sign of high energy partial discharge[8]. With its extremely low concentration distribution (usually lower than 1×10^{-5}), the detec-

*Corresponding author, E-mail address: zhangchaohai@nuaa.edu.cn.

How to cite this article: ZOU Keyuan, ZHU Min, ZHANG Chaohai. Cavity ring-down spectroscopy measurements of trace H_2S in SF_6 and SF_6/N_2 mixture[J]. Transactions of Nanjing University of Aeronautics and Astronautics, 2022, 39(S): 113-119.

http://dx.doi.org/10.16356/j.1005-1120.2022.S.015

tion device must be online and sensitive with particularly low detection limit.

Traditional way of detection, for example, GC-MS, is able to analyze the concentration of nearly all kinds of SF_6 decomposition products. However, the long injection time prevents it to be an online equipment; a variety of sensing detection methods[9-11] are introduced as well, the sensors can detect most carbonaceous components of SF_6 decomposition products[12], but for the sulfur-containing components SO_2, SOF_2, SO_2F_2 and H_2S, there are still knotty problems such as difficult desorption and long recovery time for carbon and semiconductor metal oxide sensors; Spectral methods[13] like ultraviolet fluorescence, cavity ring-down spectroscopy (CRDS)[14] and photoacoustic spectroscopy possess characteristics of high precision and stability, and they are coming into the sight of researchers. Among them, CRDS is a kind of extremely sensitive spectroscopy detection method[15-16]. As it measures the ring-down time of the laser in optical resonator instead of the light intensity, the results of the inversed concentration are anti-fluctuation of light source. Today with the advantages of high sensibility and precision, ability of real-time detection as well as no calibration required, CRDS has been widely used in field of atmospheric environmental science, biomedical science, semiconductor industry and other emerging areas.

Thus, the application of CRDS in detection of decomposition products of SF_6 in power equipment would be a practical innovation, where the decomposition component concentration is very low. To realize the detection of trace H_2S component in pure SF_6, a precise experimental platform is built to acquire the ring-down time in μs, experiments are carried out with standard gas, so that the vital absorption cross section parameters are calibrated and compared with the simulation results.

In order to deal with carbon peak and neutralization strategy, it is a trend to replace pure SF_6 with SF_6/N_2 mixture to save the amount of SF_6, because it will cause serious greenhouse effect. For this reason, this paper also discusses the inversion of H_2S concentration in SF_6/N_2 mixture as a function of mixing ratio.

1 Experiments

1.1 Experimental techniques

A simple ring-down cavity can be constructed by a pair of high-reflection mirrors (as shown in Fig.1), the reflectivity of which should be over 99.99%, so that the laser reflects thousands of times within the two mirrors before the its intensity attenuate in index to a certain threshold. The attenuation of which follows the Lambert-Beer law

$$I = I_0 e^{-\alpha l} \tag{1}$$

where I_0 and I represent the initial intensity and the transmission intensity after being absorbed by the passing medium gas, respectively. α is the absorption coefficient and l the effective absorption length.

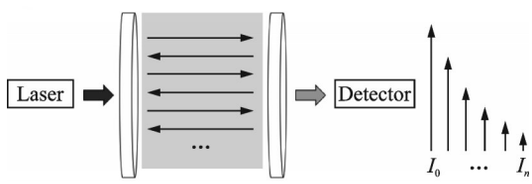

Fig.1 Schematic of absorption spectrum

The ring-down time without absorption sample is denoted as τ_0, which represents the interval in which the initial intensity I_0 attenuates to its 1/e. Due to the fingerprint absorption characteristics of spectrum, only the laser of particular wavelength can be absorbed by the gas sample, and the ring-down time will be reduced to τ. The sample concentration can thus be inversed with the following formula

$$N = \frac{1}{c\sigma(\nu)}\left(\frac{1}{\tau} - \frac{1}{\tau_0}\right) \tag{2}$$

where N is the molecular number density, c the light velocity in vacuum and $\sigma(\nu)$ the sample absorption cross section.

1.2 CRDS experimental setup

The configuration of the experimental setup is shown in Fig.2.

The light source is a distributed feedback diode laser (DFB-DL) with fiber coupling output, and the central wavelength is 1 578 nm, which corre-

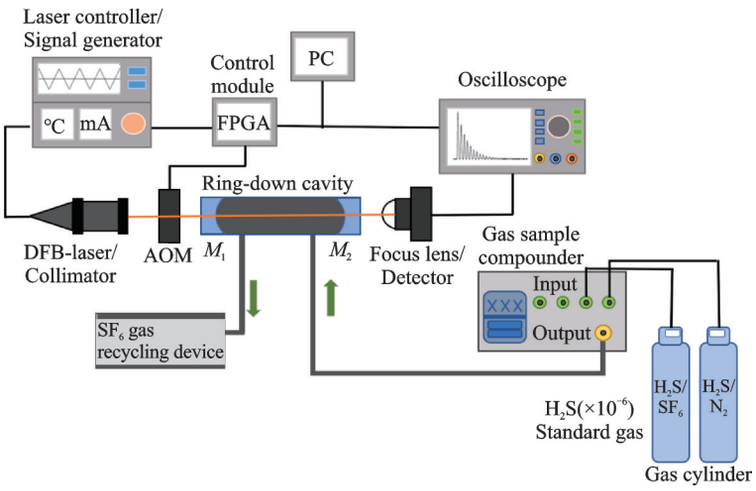

Fig.2 Schematic of CRDS experimental instrument

sponds to the obvious absorption peak around wavenumber 6 337 cm^{-1}(as shown in Fig.3). The wavelength of DFB-DL is adjusted with laser controller in Fig.2 by controlling current or temperature. The current should be in range of 30—50 mA, and the thermistor resistance is set to 10 kΩ (ambient temperature). The acousto-optic modulator (AOM) in the optical path is to cut off the laser source through frequency shift under the control of FPGA module. To ensure that the incident laser is coupled into the ring-down cavity, which is composed of a pair of high reflection mirrors M_1 and M_2 as shown in Fig.2, it is necessary to realize stable frequency matching: A triangular wave current modulation signal is loaded on the laser controller through the signal generator, with a modulation frequency of 10 Hz and an amplitude of about 50 mV. The laser beam is coupled into the ring-down cavity through collimator and optical isolator, it is added to suppress optical feedback, which may destroy the mode matching of laser and resonator.

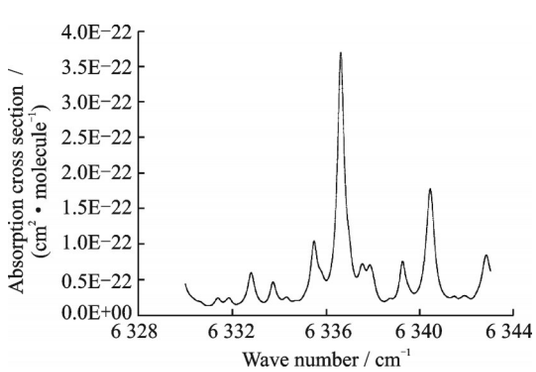

Fig.3 Absorption cross section of pure H_2S (296 K, 1 atm)

After the transmitted light passing through the second high-reflection mirror M_2, it is received by the photodetector focusing lens and collected by the oscilloscope as well as the main FPGA control module. When the transmission intensity reaches the trigger threshold, a trigger signal is generated and sent to the laser controller to turn off the laser source. The ring-down events are thus formed and the ring-down curve is recorded for subsequent data processing.

The experimental gases are standard, which are pumped into the resonant cavity after being prepared by the gas distributor. The mass flowmeter in the gas sample compunder is used to accurately monitor the outlet flow and the waste gas is recovered by special recovery device.

2 Experiment Results and Discussion

2.1 Measurements under pure carrier gas

With the experimental platform the ring-down time τ is accessible, according to Eq.(2), the absorption cross section $\sigma(\nu)$ is necessary to calculate the concentration. The convenient and widely used way is to get the $\sigma(\nu)$ from online simulation[14-17] with data of HITRAN[18-19], which is the abbreviation of high-resolution transmission molecular absorption database. It is one of the most used spectral databases in infrared spectroscopy. It is widely used for query or comparison of infrared spectral data.

The simulation results are shown in Fig.3, the profile chosen is Voigt, as the pressure 1 atm is not so high to fit Gaussian profile. The central wavenumber of the chosen peak is 6 336.62 cm^{-1}, the absorption cross section of this main absorption peak $\sigma(\nu=6\ 336.62\ cm^{-1})$ is 3.692×10^{-22} cm^2/molecule.

In order to precisely detect the concentration of the trace H_2S in SF_6 gas insulated electrical equipment, the absorption cross section $\sigma(\nu)$ of H_2S in pure SF_6 should be calibrated. Firstly 1×10^{-5} H_2S standard gas in pure SF_6 (1×10^{-5} H_2S/SF_6 in following) is pumped into the device at a flow rate of 200 ml/min. After taking the average value of multiple measurements, the ring-down time τ and the base line τ_0 of the spectrum are put into Eq.(3) to calculate the experimental value of $\sigma(\nu_0)$.

$$\sigma(\nu_0)=\frac{1}{cN}\left(\frac{1}{\tau}-\frac{1}{\tau_0}\right) \tag{3}$$

$$N=\frac{n(\times10^{-6})\cdot N_A}{22.4\times10^9} \tag{4}$$

where ν_0 is the center wavenumber automatically located by program scanning, N_A the Avogadro constant, and n ($\times10^{-6}$) the concentration parts per million. In case of 1×10^{-5} H_2S/SF_6 $\sigma(\nu_0)$ is calculated 6.293×10^{-22} cm^2/molecule, then the 5×10^{-5} H_2S/SF_6 standard gas is tested as above and the average value $\sigma(\nu_0)$ of multiple measurements turns out to be 6.367×10^{-22} cm^2/molecule, which can be considered to be consistent within the allowable error range. Thus, the $\sigma(\nu_0)$ of trace H_2S ($\times10^{-6}$ level) in pure SF_6 can be averaged as 6.330×10^{-22} cm^2/molecule, and this value is very different from the simulation value (3.692×10^{-22} cm^2/molecule). To compare the experimental calibration absorption cross section and the simulated one, 1×10^{-5} H_2S/SF_6 standard gas is diluted by SF_6 purified gas to 8×10^{-6}, 5×10^{-6}, 2×10^{-6}, respectively. As shown in the column "Trace H_2S/pure SF_6" of Table 1, the "Raw value" and corrected ones share the same ring-down time τ and τ_0, but "Raw value" is calculated with simulated $\sigma(\nu_0)$, and the "Correction value" with experimental calibrated $\sigma(\nu_0)$. Obviously, the deviation of simulation value is so large that the simulation method is almost invalid under this circumstance. Reasons can be traced back to the line broadening theory[20].

Table 1 Concentration correction with experimental calibrated absorption cross section

Concentration/10^{-6}	Trace H_2S/pure SF_6			Trace H_2S/80% SF_6, 20% N_2			Trace H_2S/50% SF_6, 50% N_2			Trace H_2S/20% SF_6, 80% N_2		
	8	5	2	8	5	2	8	5	2	8	5	2
Raw value with simulated $\sigma(\nu_0)$	13.666	8.642	3.613	5.181	3.364	1.391	2.786	2.148	0.979	2.825	1.705	0.637
Raw deviation	5.666	3.642	1.613	−2.819	−1.636	−0.609	−5.214	−2.852	−1.021	−5.175	−3.295	−1.363
Correction value	7.971	5.041	2.108	7.638	5.021	2.087	6.666	5.025	2.322	8.432	5.037	1.874
Correction deviation	−0.029	0.041	0.108	−0.362	0.021	0.087	−1.334	0.025	0.322	0.432	0.037	−0.126

In fact, the energy level of an atom is not a line without width, but has a certain frequency width. Due to various factors[21-22] (for example, natural broadening, collision broadening, Doppler broadening, etc.), the power (i.e., light intensity) of spontaneous emission/absorption is distributed in a small frequency range centered on its transition Bohr frequency ν.

$$\nu=\frac{E_2-E_1}{h} \tag{5}$$

When the frequency ν of the luminous particles deviates from the center frequency, the monochromatic light power will decay according to a certain law (profile)[23], as shown in Fig.4. And ν_0 is the center frequency.

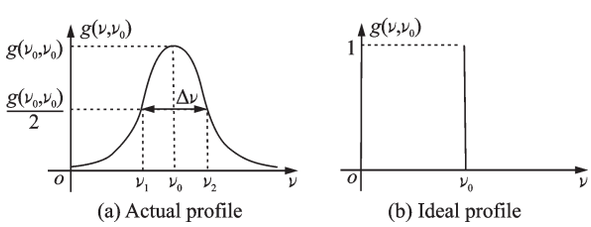

Fig.4 Spectral line broadening

The absorption cross section is proportional to the spectral profile $g(\nu)$ and absorption line strength S, which is only related to temperature and species,

and can be written as a function of temperature. It means at room temperature the line strength S of the target gas H_2S is constant. However, different carrier gas composition and their mixing ratio will affect the broadening mechanism of the spectral line, change the full width at half maximum (FWHM) $\Delta\nu$ of the profile and the function value at the central wavelength ν_0, so as to alter the absorption cross section $\sigma(\nu_0)$. The simulation is based on HITRAN database, which only involves the broadening effect of air and H_2S molecules to itself, instead of the broadening effect from the carrier gas SF_6 or the mixed carrier gas SF_6/N_2. Therefore, the simulation values in this case will cause large deviation, and the absorption cross section calibrated with standard gas is surely more accurate. At the same time, these calibrated $\sigma(\nu_0)$ also fill a tiny part of blank in the database and provide a reference for the application of CRDS in the detection of SF_6 decomposition components.

2.2 Measurements under mixed carrier gas

To calculate the concentration of trace H_2S in mixed carrier gas, standard gas with different mixing ratio of carrier is prepared and tested repeatedly to calibrate the adsorption cross section value shown in Fig.5.

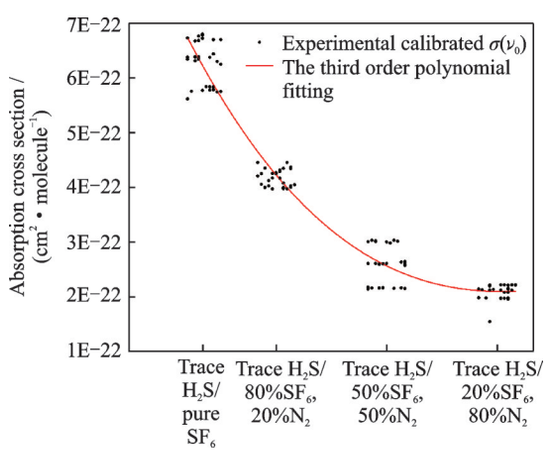

Fig.5 Variation of absorption cross section with carrier gas mixing ratio (trace H_2S in SF_6/N_2 mixture)

As the polynomial fitting curve shown in Fig.5, with the increase of the proportion of mixed nitrogen, the decrease of the $\sigma(\nu_0)$ reveals a certain regularity. Set the fitting polynomial order to 3, the analytical formula is

$$y=[2.212\,75+(-1.180\,92)x+2.326\,19x^2+2.866\,14x^3]\times 10^{-22} \quad (6)$$

where y is the central peak absorption cross section $\sigma(\nu_0)$, and x the proportion of SF_6 ($x=1$ for pure SF_6 carrier). To verify the validity of the above formula, the H_2S in the mixed carrier gas is reconfigured with the gas distributor and the concentrations are inversed with the fitted cross section data, which form the correction values in Table 1(the rest columns). The correction data is evidently much closer to the preparation standard value, and the concentrations inversed can be determined quantitatively at a precision better than 1×10^{-6}. With the subsequent verification, if the formula is applicable to other mixing ratios, the trace component detection in the case of mixed carrier gas will not need to be calibrated over and over.

3 Conclusions

An experimental platform of cavity ring-down instrument based on diode lasers using the 1 578 nm absorption band of H_2S was developed for measurements of trace H_2S in pure SF_6 and SF_6/N_2 mixed carrier gas with different mixing ratio. After calibration of the absorption cross section $\sigma(\nu_0)$ with trace H_2S standard sample in carrier gas of SF_6 and its mixture with N_2, the concentrations inversed can be determined quantitatively at a precision better than 1×10^{-6}. The corrected experimental $\sigma(\nu_0)$ is much more accurate than the simulation value, and this result also supplements some data gaps in HITRAN database. The variation of absorption cross section with carrier gas mixing ratio was studied as well, which fits well with a third order polynomial, with which the calculation of concentration in carrier gas of any mixing ratio is possible. In the field of trace gas detection CRDS is outstanding with advantages of high sensibility and precision so on, with the study and conclusions in this paper and further, its application in trace decomposition component detection of SF_6 and its gas mixture insulated electrical equipment is well expectable.

References

[1] JI Shengchang, ZHONG Lipeng, LIU Kai, et al. Research status and development of SF_6 decomposition components analysis under discharge and its application[J]. Transactions of China Electrotechnical Society, 2015, 35(9): 2318-2332.(in Chinese)

[2] LIN Tao, HAN Dong, ZHONG Haifeng, et al. Influence factors of formation of decomposition by-products of SF_6 in 50 Hz AC corona discharge[J]. Transactions of China Electrotechnical Society, 2014, 29(2): 219-225. (in Chinese)

[3] DING Weidong, OCHI K, JUNYA S, et al. Factors affecting PD detection in GIS using a carbon nanotube gas sensor[J]. IEEE Transactions on Dielectrics and Electrical Insulation, 2007, 14(3): 718-725.

[4] LUO Lishi, YAO Wenjun, WANG Jun, et al. Research on partial discharge diagnosis of GIS by decomposed gas of SF_6[J]. Power System Technology, 2010, 34(5): 225-230. (in Chinese)

[5] WANG Yu, LI Zhi, YAO Weijian, et al. Analysis of SF_6 byproducts of gas insulated switchgear (220 kV and above) in Guangdong province[J]. High Voltage Engineering, 2009, 35(4): 823-827. (in Chinese)

[6] ZHOU Yongyan, QIAO Shengya, LI Li, et al. Validity analysis of S_2OF_{10} as a target gas of partial discharge in GIS[J]. Proceedings of the CSEE, 2016, 36(3): 871-878. (in Chinese)

[7] TANG Ju, YANG Dong, ZENG Fuping, et al. Research status of SF_6 insulation equipment fault diagnosis method and technology based on decomposed components analysis[J]. Transactions of China Electrotechnical Society, 2016, 31(20): 41-54. (in Chinese)

[8] TANG Nian, QIAO Shengya, LI Li, et al. Validity of HF and H_2S as target gases of insulation monitoring in gas insulated switch gear[J]. Transactions of China Electrotechnical Society, 2017, 32(19): 202-211. (in Chinese)

[9] ZHANG Xiaoxing, FANG Jiani, CUI Hao, et al. Review: Adsorption principle and application of carbon nanotubes to SF_6 decomposition components[J]. Proceedings of the CSEE, 2018, 38(16): 4926-4941, 4997. (in Chinese)

[10] YU Lei. Gas sensitivity properties and sensing mechanism Studies on pristine and gold modified graphene detecting SF6 decomposed components[D]. Chongqing: Chongqing University, 2015. (in Chinese)

[11] ZHANG Xiaoxing, HUANG Rong, YU Lei, et al. Gas sensing analysis properties of Au-graphene to SF_6 decomposition products based on a first principle study[J]. Proceedings of the CSEE, 2017, 37(6): 1828-1835. (in Chinese)

[12] NERI G, LEONARDI S G, LATINO M, et al. Sensing behavior of SnO_2/reduced graphene oxide nanocomposites toward NO_2[J]. Sensors and Actuators B: Chemical, 2012, 179: 61-68.

[13] ZHANG Xiaoxing, YIN Zhang, TANG Ju, et al. Optical technology for detecting the decomposition products of SF_6: A review[J]. Optical Engineering, 2018, 57(11): 110901-1-110901-12. (in Chinese)

[14] SONG Shaoman. Continuous wave cavity ring-down spectroscopy device and trace methane detection[D]. Changchun: Chinese Academy of Sciences, 2019. (in Chinese)

[15] ZHANG Chaohai, SHI Huixuan, QIN Zhaoyu, et al. CRDS based SF_6 decomposition detection technology for SF_6 electrical equipment[J]. Southern Power System Technology, 2016, 10(5): 68-74. (in Chinese)

[16] WALKER S A, AZETSU-SCOTT K, NORMANDEAU C, et al. Oxygen isotope measurements of seawater ($H_2^{18}O$/ $H_2^{16}O$): A comparison of cavity ring-down spectroscopy (CRDS) and isotope ratio mass spectrometry (IRMS)[J]. Limnology and Oceanography: Methods, 2016. DOI.10.1002/lom3.10067.

[17] MA Dongxing. Study on the cavity ring down spectroscopy in trace gas concentration measurement[D]. Nanjing: Southeast University, 2017. (in Chinese)

[18] KARPF A, RAO G N. Enhanced sensitivity for the detection of trace gases using multiple line integrated absorption spectroscopy[J]. Applied Optics, 2009, 48(27): 5061-5066.

[19] ROTHMAN L S, GORDON I E, BARBE A, et al. The HITRAN, 2008 molecular spectroscopic database[J]. Journal of Quantitative Spectroscopy and Radiative Transfer, 2009, 110(9): 533-572.

[20] OUYANG Xiang, VARGHESE P L. Reliable and efficient program for fitting Galatry and Voigt profiles to spectral data on multiple lines[J]. Applied Optics, 1989, 28(8): 1538-1545.

[21] CHESKIS S, DERZY I, LOZOVSKY V A, et al. Cavity ring-down spectroscopy of OH radicals in low pressure flame[J]. Applied Physics B, 1998, 66(3): 377-381.

[22] RINSLAND C P, DEVI V M, SMITH M, et al. Measurements of air-broadened and nitrogen-broadened Lorentz width coefficients and pressure shift coefficients in the Nu4 and Nu2 bands of $C_{12}H_4$[J]. Applied Optics, 1988, 27(3): 631-651.

[23] BOONE C D, WALKER K A, BERNATH P F.

Speed-dependent Voigt profile for water vapor in infrared remote sensing applications[J]. Journal of Quantitative Spectroscopy and Radiative Transfer, 2006, 105(3): 525-532.

Acknowledgements This work was supported in part by the National Key R&D Program of China (No.2021YFF0603100), and in part by the Leading Innovation and Entrepreneurship Team in Zhejiang Province (No.2019R01014).

Authors Miss **ZOU Keyuan** received the B.S. degree in electrical engineering and automation in 2019 from Nanjing University of Aeronautics and Astronautics, Nanjing, China. She is currently pursuing the M.S. degree in electrical engineering in Nanjing University of Aeronautics and Astronautics. Her research area is intelligent diagnosis of high-voltage equipment.

Prof. **ZHANG Chaohai** received the B.S. degree at Harbin Industrial University, M.S. degree from Naval Aeronautical Engineering Institute and the Ph.D. degree Hong Kong Polytechnic University. He is currently a professor in College of Automation from Nanjing University of Aeronautics and Astronautics. His research areas are gas insulation, intelligent electrical equipment and pulse power and plasma technology.

Author contributions Miss **ZOU Keyuan** designed this research, compiled the model, conducted the simulation and the experiments, analyzed the results, and wrote the manuscript. Prof. **ZHANG Chaohai** and Dr. **ZHU Min** contributed to the background and modification of the final paper. All authors commented on the manuscript draft and approved the submission.

Competing interests The author declares no competing interests.

(Production Editor: SUN Jing)

光腔衰荡光谱法检测SF_6以及SF_6/N_2混合载气下的痕迹H_2S

邹可园，朱　珉，张潮海

(南京航空航天大学自动化学院，南京 211106，中国)

摘要：H_2S是六氟化硫绝缘气体最重要的特征组分之一，痕迹H_2S的检测对SF_6气体绝缘电气设备的早期故障诊断具有重要意义。为监测SF_6和SF_6/N_2混合载气中H_2S的浓度，本文研制了基于1 578 nm波长分布反馈二极管激光器(Distributed feedback diode laser，DFB-DL)的腔衰荡光谱(Cavity ring-down spectroscopy，CRDS)实验平台，其检测灵敏度优于1×10^{-6}。吸收截面参数σ对于计算浓度至关重要，使用标准气体样品进行重复实验，标定了纯SF_6和不同混合比的SF_6/N_2混合载气中H_2S的σ参数，并通过与σ仿真值的比较讨论了载气对谱线展宽的影响。研究了吸收截面σ参数随载气混合比的变化规律，从而可以计算任意混合比载气下的目标气体浓度。由此，CRDS在气体绝缘电气设备痕量成分检测中的应用前景十分可观。

关键词：腔衰荡光谱；吸收截面；H_2S；SF_6分解组分